Chemical Physics Letters 601 (2014) 116–123

Contents lists available at ScienceDirect

Chemical Physics Letters

journal homepage: www.elsevier.com/locate/cplett

Theoretical study of the reaction mechanism of a series of 4-hydroxycoumarins against the DPPH radical

Sergio A. Rodríguez [a], Maria T. Baumgartner [b,*]

[a] CITSE (CONICET), Instituto de Química Orgánica, Facultad de Agronomía y agroindustrias, Universidad Nacional de Santiago del Estero, Av. Belgrano Sur 1912, Santiago del Estero 4200, Argentina
[b] INFIQC (CONICET), Dpto. de Química Orgánica, Facultad de Ciencias Químicas, Universidad Nacional de Córdoba, Ciudad Universitaria s/n, Córdoba 5000, Córdoba, Argentina

ARTICLE INFO

Article history:
Received 5 November 2013
In final form 27 March 2014
Available online 4 April 2014

ABSTRACT

Structural, electronic and energetic characteristics of a series of 4-hydroxycoumarin derivatives have been studied using DFT to elucidate the mechanisms involved in their antiradical activities against DPPH radical. Different mechanisms were examined. The thermodynamic parameters obtained were BDE, IP, ETE, PA and PDE, both in gas and methanolic phase. The evaluation of these parameters allowed to conclude that the most probable mechanism was HAT. In addition, the transition state (TS) and pre-TS complex for the reaction of hydroxycoumarins and DPPH· were calculated. The results provide a physicochemical understanding of the hydrogen abstraction of a no-phenolic hydroxyl.

1. Introduction

The nitrogen-centered radical DPPH· (2,2-diphenyl-1-picrylhydrazyl) has been extensively employed in the studies of hydrogen atom abstraction particularly from phenols (ArOH) [1]. The following advantages of employing this radical should be highlighted here: it is commercially available, air stable and strongly colored, allowing the course of reaction to be monitored using UV–vis spectroscopy [2].

It is now known that the H-atom abstractions from phenols by free radical DPPH may occur through different mechanisms [3] in which an electron and a proton are transferred a) in a single step (hydrogen-atom transfer (HAT) or proton-coupled electron-transfer (PCET) [4]) or b) in two steps (sequential proton-loss electron-transfer (SPLET) [1d,e] and electron-transfer proton-loss (ET-PT) [5]). From the antioxidant action viewpoint, the result of the different mechanisms is the same that is the phenoxide radical formation.

In the HAT mechanism, a hydrogen atom of OH group is transferred from phenol (ArOH) to free radical DPPH, resulting in the formation of a phenoxyl radical (ArO·) and the DPPH-H molecule (Eq. (1)) [3]. Bond dissociation energy (BDE) has been used as an energetic parameter to evaluate the feasibility of this mechanism [6]. Therefore the compound that has the weakest OH bond reacts more quickly with free radicals.

$$\mathrm{ArOH} + \mathrm{DPPH}^{\cdot} \xrightarrow{\mathrm{HAT}} \mathrm{ArO}^{\cdot} + \mathrm{DPPH\text{-}H} \quad (1)$$

PCET mechanism has been proposed based on theoretical studies since it cannot be experimentally differentiated from HAT [4]. In the HAT mechanism, the proton together with one of its two bonding electrons are transferred to the radical. In the PCET mechanism, the proton and electron go to different acceptors. The proton moves between two electron pairs and the accompanying fifth electron moves between nonbonding orbitals [3]. Using theoretical calculations, Foti et al. [7] showed that the reaction of phenols with DPPH radical, where the structure of TS complex has no symmetry, occurs via a single pathway by a mechanism that has both HAT and PCET character.

$$\mathrm{ArOH} \longrightarrow \mathrm{ArO}^{-} + \mathrm{H}^{+} \quad (2)$$

$$\mathrm{ArO}^{-} + \mathrm{DPPH}^{\cdot} \longrightarrow \mathrm{ArO}^{\cdot} + \mathrm{DPPH}^{-} \quad (3)$$

Eqs. (2) and (3) describe the SPLET mechanism, where a proton is first lost by an acid-base equilibrium to give the phenoxide anion followed by an electron transfer from these species to form the phenoxyl radical and DPPH anion [1d,e].

Proton affinity (PA) can be used as an efficient thermodynamic parameter to evaluate the proton loss from aromatic alcohol; the lower PA, the easier the heterolytic bond cleavage will be. The second step in SPLET mechanism, the formation of phenoxyl radical from a single electron transfer for phenoxide anion, can be evaluated by electron transfer energy (ETE).

In ET-PT mechanism [5], the first step is the electron transfer from the aromatic alcohol to DPPH· (Eq. (4)) to form a radical cation and DPPH anion, this process being characterized by calculating the ionization potential of the neutral molecule (IP). The second

* Corresponding author.
E-mail address: tere@fcq.unc.edu.ar (M.T. Baumgartner).

http://dx.doi.org/10.1016/j.cplett.2014.03.080
0009-2614/

step consists in the proton transfer from radical cation of alcohol to DPPH anion giving the corresponding neutral radical (Eq. (5)).

$$ArOH + DPPH^{\cdot} \longrightarrow ArOH^{\cdot+} + DPPH^{-} \quad (4)$$

$$ArOH^{\cdot+} + DPPH^{-} \longrightarrow ArO^{\cdot} + DPPH\text{-}H \quad (5)$$

SPLET and ET-PT mechanisms have a strong dependence on the solvent nature due to the formation of charged species, as opposed to HAT and PCET.

In previous articles we reported the synthesis of a series of 4-hydroxycoumarins [8] and the study of their antiradical activity against DPPH radical, ABTS cation radical and an enzymatic system (LOX, lipoxigenase) that promote the co-oxidation of linoleic acid and β-carotene [9]. Furthermore, a preliminary theoretical study of reaction mechanism of synthetic 4-hydroxycoumarins and DPPH· was shown. It is important to remark that most antioxidants theoretical works employ phenols type compounds but the 4-hidroxycoumarins are not phenols; the OH group is bonded at a vinylic carbon.

The aim of this work was to study the mechanistic behavior of these series of 4-hidroxicoumarins (no-phenolic antioxidant) against DPPH radical, employing theoretical calculations to interpret the experimental results obtained, and to compare the results with the known behavior of phenols with DPPH·. We calculated the structures of the species that participated in each mechanism, using DFT calculations. We obtained the different thermodynamic parameters (BDE, PA, IP, ETE) in order to discern the mechanism of action of this family. Furthermore, the SPLET and ET-PT mechanisms are of importance in solution-phase, so it is interesting to ascertain how the solvent alters the reaction enthalpies of individual steps of the three mechanisms.

2. Materials and methods

2.1. Theoretical calculations

All calculations reported in the present study were carried out employing the density functional theory, as implemented in the Gaussian 03 package [10]. B3LYP[11] level of density functional theory was used. The geometry of radicals ($ArO^{\cdot}$), neutral species (ArOH), anions (ArO^{-}) and radical cations ($ArOH^{\cdot+}$) was fully optimized at the B3LYP/6-31G(d) level of theory. In the computations, no constrains were investigated. All structures were true minima on the calculated potential surface, verified by frequency calculations. Vibrational frequencies were computed at the same level of theory for all the optimized structures.

The enthalpy (ΔH_f) was obtained by thermal correction to the electronic energy by adding zero-point energy (ZPE), translational, rotational, and vibrational contribution. All enthalpies were calculated for 298.15 K and 1.0 atmosphere pressure (101.325 kPa). For the enthalpy of H^+ and e^- we used enthalpy values reported (1.48 and 0.75 kcal/mol) [12].

The solvent effects were also computed using the polarizable continuum model (IEF-PCM) [13]. The solvent used was methanol. For the enthalpy $H^{\cdot}$, H^+ and e^- calculations in methanol we used the hydration energy corrections reported (1.2, −248.09 and −20.6 kcal/mol) [12].

Since Gaussian 03 allows solution-phase geometry optimization, this approach was used for the parent molecules and their respective radicals, radical cations and anions.

The atoms of the compound have been numbered as shown for **4** in Figure 1.

The reaction coordinate calculations were carried out using DFT with Gaussian 09 package of programs [14]. The geometry of the TS, complexes pre-TS and products between DPPH· and coumarins was fully optimized at the (U)B3LYP/6-31G(d) level. Each TS was confirmed to have only one imaginary vibrational frequency mode.

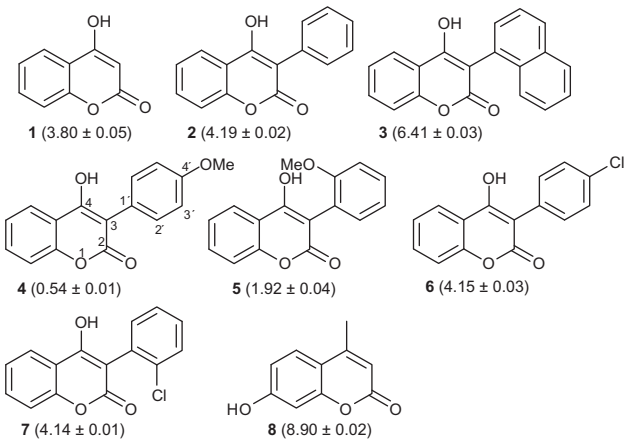

Figure 1. Chemical structures of the studied coumarins and EC_{50} values in mM.

3. Results and discussion

Six 4-hydroxy-3-aryl-coumarins were selected to study their antioxidant activities taking as reference the unsubstituted 4-hydroxycoumarin. Besides, 7-hydroxy-4-methylcoumarin (4-methylumbelliferone) was also measured to compare the reactivity between 4-hydroxy and 7-hydroxycoumarins (vinylic and phenolic OH, respectively). Figure 1 shows the chemical structures of the studied compounds and the antiradical activity found against DPPH· expressed as EC_{50} values [15] in mM [9].

The increasing activity order observed in this system (inverse to the EC_{50} values) was **8** < **3** < **7**∼**6**∼**2** < **1** < **5** < **4**. The compounds bearing *o*- and *p*-OMe groups as substituent of the aryl ring in C_3 had the highest activity whilst the lowest one corresponded to 4-methylumbelliferone.

3.1. Structural analysis

In this study, the most stable conformer has been used for all species (Figure S1) [16]. In Table 1 some important structural parameters of neutral and radical species are listed.

The O–H and C–O distances are very similar for different neutral compounds. In a similar way, the C–O–H angles are conserved.

The twist angle (between the cycles) of 3-aryl substitute molecules changed when the group in the aryl moiety was in *ortho* or *para* position. In the *para* phenyl substitutes molecules (**4**, **6**) this angle was similar to 3-phenyl-4-hydoxycoumarin (**2**). In derivate **7**, the *o*-chlorophenyl ring is more rotated out of the plane of coumarin ring due to repulsion between OH and chlorine group (see Figure S2 in supplementary material).

Moreover, in search of the lowest energy structure of compound **5**, it was found that it presents an intramolecular hydrogen bond between O of OCH_3 group and H of O–H bond with a distance of 1.7274 Å.

One notorious change was observed when comparing the C–O distances and the twist angles of neutral and radical molecules. In the neutral molecules these angles are more displaced from coplanarity than in radical species, this behavior is accentuated when the geometrical optimizations were performed in solvent. However, this was not observed for the radical of **5** due to the repulsion between the O of OCH_3 and O at C_4 (Figure S3).

Table 1
Structural parameters of neutral and radical species in gas and solvent phase.[a]

Compound	*R*(O–H) Å	*R*(C–O) Å	Twist angle (4-3-1′-2′)	H–C–O angle; H–O–C_4–C_3 angle
1	0.971 (0.993)	1.352 (1.339)		109.3 (110.9); 0.0 (0.0)
1·		1.238 (1.238)		
2	0.976 (0.982)	1.350 (1.344)	−49.5 (−56.9)	108.6 (111.4); −2.7 (−10.1)
2·		1.236 (1.239)	−27.3 (−32.8)	
3	0.977 (0.983)	1.349 (1.342)	−65.1 (−70.7)	107.9(111.5) −1.0 (5.2)
3·		1.237 (1.241)	−41.9 (−44.7)	
4	0.976 (0.982)	1.351 (1.344)	−49.4 (−61.3)	108.4 (111.1); −3.6 (−9.8)
4·		1.237 (1.241)	−22.6 (−28.7)	
5	0.983 (0.986)	1.345 (1.342)	−47.8 (−49.4)	108.3 (108.6); −28.9 (−28.9)
5·		1.233 (1.236)	−45.2 (−47.6)	
6	0.975 (0.982)	1.350 (1.343)	−48.9 (−56.5)	108.8 (111.7); −3.7 (−11.71)
6·		1.236 (1.239)	−25.3 (−31.9)	
7	0.975 (0.984)	1.349 (1.341)	−110.6 (−108.6)	108.5 (112.2); −0.4 (7.8)
7·		1.236 (1.238)	−133.5 (−131.3)	
8	0.970 (0.990)	1.361 (1.354)		109.4(110.6); 0.0 (0.0)
8·		1.251 (1.255)		

[a] Between parentheses the values found by optimization in methanol.

The substitution in C_3 of **1** with a series of substituted aryl groups did not modify the electrostatic potential or unpaired spin distribution, either in gas phase or in solution (Figure S3 and S4).

3.2. HAT mechanism

As mentioned in the introduction, the HAT mechanism corresponds to the homolytic dissociation of an O–H bond. This mechanism depends on two bond dissociation enthalpies (BDE), the O–H BDE of ArOH and the H-R BDE of the radical DPPH. The O–H BDE can be calculated by the following equation [6]

$$BDE_{ArO-H} = \Delta H_f(ArO^{\cdot}) + \Delta H_f(H^{\cdot}) - \Delta(ArOH) \quad (6)$$

where $\Delta H_f(ArO^{\cdot})$ is the enthalpy of formation of the hydroxycoumarin radical generated after H-abstraction, $\Delta H_f(H^{\cdot})$ is the hydrogen atom, and $\Delta H_f(ArOH)$ is the enthalpy of formation of the antioxidant molecule.

In this work, BDE of studied compounds were determined using three approaches. In the first, BDE were evaluated from the calculated total electronic energies, E_0 (BDE_{E0}). The main reason of this approach application was the effort to omit any corrections. Moreover, the plausibility of this hypothesis has been confirmed for a large number of phenols, tocopherols and chromans [17]. In the second approach, BDE were calculated on the basis of Eq. (6) to obtain gas phase values at 298 K. Finally, BDE (BDE_S) were calculated taking into account the influence of solvent (MeOH) performing the full optimization of the structures. Table 2 summarizes the BDE_{E0}, BDE and BDE_S obtained.

The gas phase BDE are lower than the BDE_{E0} values by 6–7 kcal/mol but the relative energy (ΔBDE) between the substituted coumarins (**2–7)** with respect to **1** have the same order in both cases. This fact can also be reflected in Figure S5, showing an excellent correlation between these parameters. These results clearly show that there is no need to make corrections to the electronic energy to obtain BDE tendency. The BDE order is **4** < **6** < **2** < **3** < **5** < **7** < **8** < **1**.

In phenolyc antioxidants, experimental and theoretical results indicate that the ring substituents changed the BDE and any substituent destabilizing the phenol (ground-state effect), and/or stabilizing the phenoxyl radical (radical effect). The *ortho* and *para* electron-donating (ED) groups decrease the BDE_{OH} and increase the reactivity [6,18].

In the coumarins family, the substituent effect was analyzed. Figure 2 shows the stabilization energy (E_{H-Ar}) of the neutral molecule given by the interaction between H of OH and 3-aryl ring. In **2**, the presence of phenyl group at C_3 interacting with OH stabilizes the neutral molecule in 5.72 kcal/mol relative to non-interacting structure (Figure 2).

Furthermore, the substituents on *para* position of the phenyl group at C_3 show a similar effect to that observed when they are directly bonded to the phenol [6,18]. When the substituent in *para* is a donor, the overall effect is a decrease of the O–H BDE. The OMe and Cl group decreases BDE with respect to **2** in 3.08 and 0.6 kcal/mol, respectively (for fenol *p*-OMe = 4.4 kcal/mol and *p*-Cl = 0.4 kcal/mol, respectively) [18].

In **4** and **5**, the O–C bond of the methoxy group is coplanar with the phenyl ring to which it is attached, comparable with phenol compounds [18]. In this conformation the overlapping of the lone pair of ϑ-symmetry is optimized and the maximum electron-donating effect occurs (Figure S6). The effect of *o*-methoxy group would be essentially the same as that of a *p*-methoxy group [19]. However, the presence of O-alkyl groups near OH involves the intramolecular hydrogen bond formation in neutral species. In compound **5**, *ortho* methoxy group increased the BDE value 6.60 kcal/mol compared to **4.** This is due to different contributions including E_{H-Ar}, hydrogen intramolecular bond and steric effect (see Figure 2).

If we compare the BDE of **6** and **7**, the difference is 4.55 kcal/mol. This value will be considered a measure of the alteration of the BDE only due to different position of the chlorine atom (see Figure S7).

In the solvent, there is a difference between the gas phase O–H bond dissociation enthalpies ranging from 1.5 to 7.9 kcal/mol higher than gas phase values as given in Table 2.

When comparing the BDE obtained in the gas phase and solvent, the correlation was not so good (Figure S5). The BDE in the gas phase predict the following order of decreasing activity **4** > **6** > **2** > **3** > **5** > **7** > **8** > **1**, while BDE_S shows the following order **4** > **2** > **6** > **5** > **3** > **7** > **8** > **1**. This indicates the need to assess the relation between BDE and the activity found. In order to analyze this behavior the activity (EC_{50}) as a function of BDE_{E0} and BDE_S (Figure 3a and b respectively) was plotted. In these plots we found a very good correlation between activity and BDE for *p*-substituted phenyl coumarin family, both in gas phase and solvent. However, four compounds deviated from this correlation **1**, **8**, **5** and **7**.

Table 2
BDE, PA, ETE, IP and PDE values of hydroxycoumarin derivatives.[a]

Compound	BDE_{E0}[b]	BDE[c]	ΔBDE	BDE_S[d]	ΔBDE_s	PA[e]	PA_S[f]	ETE[g]	ETE_S[h]	IP[i]	IP_S[j]	PDE[k]	PDE_S[l]
1	88.50	81.44	0	89.37	0	330.09	42.65	66.03	91.43	188.22	124.17	207.90	10.00
2	82.66	75.98	−5.47	79.51	−9.86	326.78	40.02	63.87	84.21	172.79	112.67	217.86	11.63
3	85.28	78.51	−2.93	81.28	−8.09	328.12	41.19	65.07	84.81	166.81	109.11	226.38	16.97
4	79.37	72.90	−8.54	76.10	−13.27	327.96	40.50	59.61	80.32	162.76	105.61	224.81	15.29
5	86.34	79.51	−1.94	80.76	−8.60	332.45	47.03	61.73	78.45	165.39	110.88	228.78	14.68
6	82.03	75.38	−6.07	79.73	−9.64	321.30	38.17	68.75	86.28	174.07	113.80	215.98	10.73
7	86.77	79.93	−1.51	84.18	−5.19	326.49	43.97	68.12	84.93	177.72	118.64	216.89	10.33
8	87.41	80.41	−1.04	85.58	−3.79	336.19	51.81	58.90	78.59	179.28	114.08	215.80	16.39

[a] All values are expressed in kcal/mol.
[b] $BDE_{E0} = E_0(ArO\cdot) + (-0{,}50027\ hartree) - E_0(ArOH)$.
[c] $BDE = H(ArO\cdot) + (-0{,}49791 hartree) - H(ArOH)$.
[d] $BDE_S = H_S(ArO\cdot) + (-0.49837 hartree) - H_S(ArOH)$.
[e] $PA = H(ArO^-) + 1.48\ kcal/mol - H(ArOH)$.
[f] $PA_S = H_S(ArO^-) - 246{,}6\ kcal/mol - H_S(ArOH)$.
[g] $ETE = H(ArO\cdot) + 0.75\ kcal/mol - H(ArO^-)$.
[h] $ETE_S = H_S(ArO\cdot) - 19.85\ kcal/mol - H_S(ArO^-)$.
[i] $IP = H(ArO^{\cdot+}) + 0.75\ kcal/mol - H(ArOH)$.
[j] $IP_S = H_S(ArO^{\cdot+}) - 19.85\ kcal/mol - H_S(ArOH)$.
[k] $PDE = H(ArO\cdot) + 1.48\ kcal/mol - H(ArO^{\cdot+})$.
[l] $PDE_S = H_S(ArO\cdot) - 246.6\ kcal/mol - H_S(ArO^{\cdot+})$.

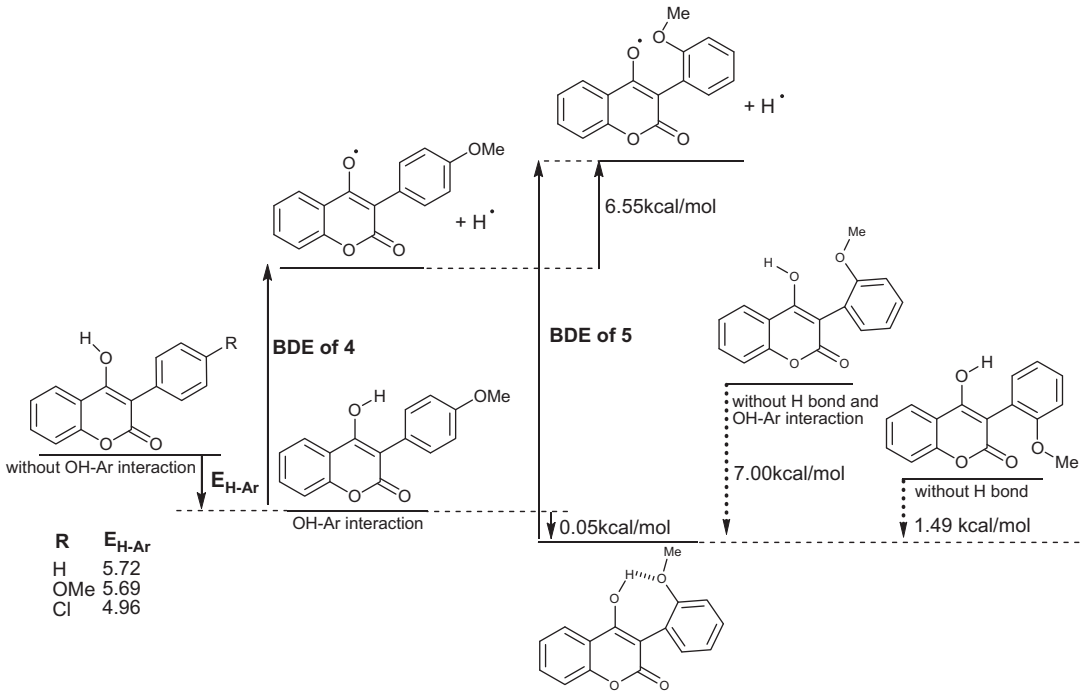

Figure 2. Stabilization energies ($E_{H\text{-}Ar}$) of neutral *p*-substituted molecules and the comparison of *ortho* or *para* substitution.

Reaction 1 is endothermic for many phenols [7]. Similar results were observed for the coumarin family. The enthalpy of reaction 1 is 7.90 kcal/mol for **1**, 2.43 kcal/mol for **2**, 1.83 kcal/mol for **6** and 6.38 kcal/mol for **7**, in gas phase. In solvent, the values decreased and some are exothermic (6.35 kcal/mol for **1**, −3.32 kcal/mol for **2**, −3.10 kcal/mol for **6** and 1.34 kcal/mol for **7**) but the relative order is the same. The steric accessibility of the DPPH· radical is a major determinant of the reaction, since small molecules that have better access to the radical site have relatively higher antioxidant capacity.

Ortho substituted compounds exhibit a lower activity related with their BDE than the corresponding *para* substituted similarly to those observed in phenols, and consequently a different relationship BDE vs. activity [20]. So, for this family of molecules a relationship can be established taking into account two main factors: the substituents and the steric effect.

3.3. SPLET mechanism

The SPLET mechanism is operative in solvents that support ionization, such as alcohols and water. The ArOH may be in equilibrium with the corresponding anion ArO^-, which is a much stronger electron donor as compared to the parent ArOH.

In order to study the feasibility of SPLET mechanism, the proton affinity (PA) and the electron transfer energy (ETE) values (Eqs. (7), (8)) were calculated. In the same way as for BDE, the electronic energies (PA_{E0} and ETE_{E0}), enthalpies (PA and ETE) and solvent optimizations (PA_S and ETE_S) were considered (Table 2).

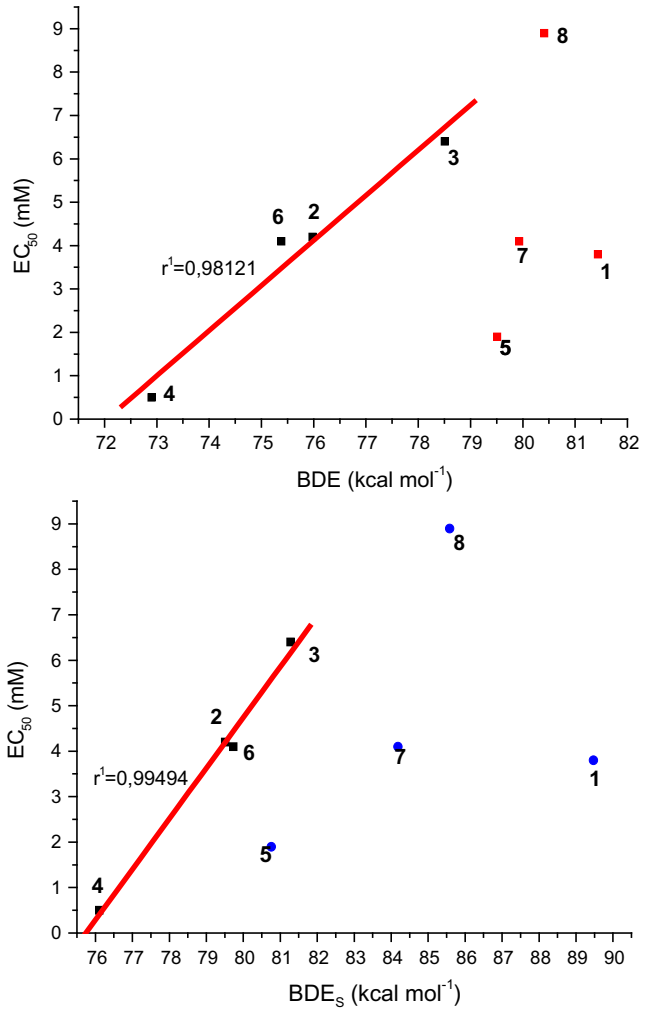

Figure 3. (a) EC_{50} vs BDE. (b) EC_{50} vs BDE_s.

$$PA_{ArO-H} = \Delta H_f(ArO^-) + \Delta H_f(H^+) - \Delta H_f(ArOH) \quad (7)$$

$$ETE_{ArO-H} = \Delta H_f(ArO^{\cdot}) + \Delta H_f(e^-) - \Delta H_f(ArO^-) \quad (8)$$

In the case of proton affinities, the calculation results could be compared with the experimental values of **1** and **8**, and we observed the same trend (**8** > **1**) [21].

In the gas phase the limiting step of SPLET mechanism will be the one governed by the proton affinity. If the process has the energy to deprotonate the hydroxycumarin, the electron transfer step should occur easily.

Excellent correlations in the plot between PA_{E0}/PA and ETE_{E0}/ETE values (see Supporting information, Figure S8) were found, indicating that it is not necessary to introduce energy corrections to E_0 values.

PA_{E0} and PA in the gas phase predict the following increasing order of activity **8** > **5** > **1** > **3** > **4** > **2** > **7** > **6**. This order does not correlate with the experimental results. Even more, the plots of PA or PA_{E0} vs EC_{50} do not present a clearly tendency (see Supporting). This lack of correlation and the fact that BDE obtained in the gas phase were lower than PA, lead to the conclusion that, in this phase, the HAT mechanism probably represents the main path to explain the experimental behavior.

On the other hand, the SPLET mechanism is important in solvents, so it is interesting to see how the enthalpies change in this medium. PA results are similar to the gas phase indicating that the deprotonation of **2** is easier than the one of **1** and the latter more than those of **8** and **5.**

In the methanolic phase the limiting step of SPLET was governed by ETEs values. The process of deprotonation of compounds was favored compared with the electron transfer process. ETEs predict the following decreasing order of activity **8**∼**5** > **4** > **2** > **3** > **7** > **6** > **1**. The order does not correspond with the experimental, and the plot EC_{50} vs ETEs do not show any correlation (Figure S8).

The first experimental analyses to establish the differences between HAT and SPLET mechanisms were those reported by Litwinienko and Ingold, and Foti et al. [1b,c]. They found that the reaction rates of different phenols towards DPPH· were modified by adding different concentrations of acetic acid to the system, the reaction being generally slower.

In order to evaluate the influence of SPLET mechanism in the global reactivity of the hydroxycoumarin family against DPPH·, the EC_{50} values for **1**, **3** and **5** were determined with the addition of acetic acid to final concentration of 10 mM and 100 mM [22]. The EC_{50} value of compounds was slightly modified in both cases (10 mM EC_{50} increases 4% and 100 mM EC_{50} increases 6%) with respect to the EC_{50} without any addition (in the standard conditions of system). This experiment allows determining the contribution of SPLET mechanism to the global reaction, being this participation of about 5%.

The experimental determination and theoretical calculations show the HAT pathway as the primary mechanism of the reaction of hydroxycoumarins with DPPH· in the present experimental conditions, even for hindered compounds.

3.4. ET-PT mechanism

The ET-PT mechanism and was evaluated by analyzing the ionization potential (IP) and proton dissociation energy (PDE).

$$IP_{ArO-H} = \Delta H_f(ArOH^{+\cdot}) + \Delta H_f(e^-) - \Delta H_f(ArOH) \quad (9)$$

$$ETE_{ArO-H} = \Delta H_f(ArO^{\cdot}) + \Delta H_f(H^+) - \Delta H_f(ArO^{+\cdot}) \quad (10)$$

Table 2 summarizes the IP and PDE values calculated by following the same approximations that were used with the other parameters.

Again, the calculated parameters using enthalpies perfectly correlate with those obtained with E_0 energies, but not as well as with the calculated values in the solvent.

The IP values indicate that the molecule does not lose electrons easily. **1** was found to be the least active in the ET reaction (Eq. (4)) while the most active are **4** and **5**. The IP values are higher than BDE in every calculation.

The calculated values show that the ET (Eq. (4)) is endothermic stage, while proton transfer (Eq. (5)) is exothermic both in solvent as in gas phase [23]. PDE is therefore a determining step in this mechanism.

The IP and PDE calculated do not show a correlation with the EC_{50} values (see Figure S9). Hence, this mechanism may not operate in the reaction.

3.5. Reaction path

Using theoretical calculations of the transition state, different mechanisms (HAT or PCET) for the reaction of phenols and DPPH radical have been proposed [7].

We studied the reaction path between DPPH· and the coumarins family. Exhaustive search of conformational space was not preformed, but, due to great steric hindrance in the radical center (N· of DPPH) to interact with coumarins, the spatial conformations are limited and the results of this approach are relevant. Some

important structures were obtained, a pre-transition state (pre-TS) and TS. A few conformations of pre-TS were studied and the reaction coordinate was performed from the most stable of them. The calculations indicate that the reaction proceeds in one step and via a single TS structure (Figure 4).

The pre-TS have a hydrogen bond between the hydrogen of OH and a lone pair on N of DPPH. This bond in pre-TS causes the O atom and the radical center to approach more closely than they would if a bond was not formed.

In the reaction between DPPH· and **4**, the most active compound was taken as reference (Figure 4). In pre-TS complex, we observed that the *R*(H–N) distance is 2.2576 Å and *R*(O–H) is 0.9785 Å (Table 3). The calculations predict that the OH group of the hydroxycoumarin remains essentially in the same plane of the coumarin ring, φ (H–O–C_4–C_3) = −11.1°. Moreover, the hydroxycoumarin ring is oriented roughly perpendicular to the plane defined by C–N·–N of DPPH. The effect of steric congestion in the DPPH radical can be observed in the values obtained for torsion and dihedral angles, which deviate from the ideal value [24]. Thus, the torsion angle corresponds to hydrogen bond, θ (O–H–N·) has a value of 140.8°, and this is 39.2° deviated from the ideal values. Similar geometric parameters were found for preTS complexes of **2** and **6**.

In the TS of **4**, the *R*(H–N) distance is 1.2512 Å and *R*(O–H) is 1.2315. The higher steric hindrance in the TS is responsible for φ (H–O–C_4–C_3) = −58.2° ('ideal' 0° for PCET, 90° for HAT) [7,25] and 47.1° more deviated than in pre-TS. These results provide evidence that both mechanisms (HAT and PCET) may be taking place for this family of vinyl alcohols similar to what happens with the phenols [7], being HAT predominant.

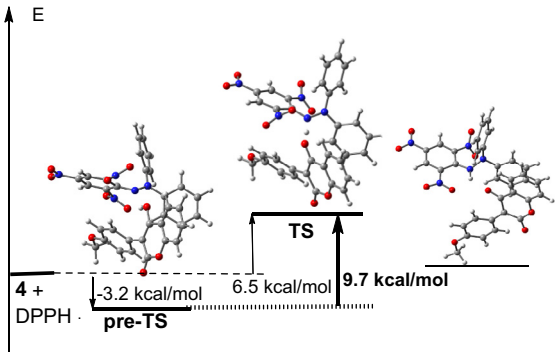

Figure 4. Reaction path of **4** and DPPH·.

For phenols compounds, $R(O–H)_{TS}$ and $R(H–N)_{TS}$ vary synchronously in a correlative manner with σ_p^+. As σ_p^+ decreases, $R(O–H)_{TS}$ and $R(H–N)_{TS}$ decrease and increase, respectively [26]. We interestingly observed that the *para* substituted compound shows a similar correlation with respect to **2** (Figure S10). For **4** ($\sigma_p^+ = -0.78$) [27], smaller $R(O–H)_{TS}$ and larger $R(H–N)_{TS}$ are observed (1.2315 and 1.2512 Å, respectively). And for **6**, ($\sigma_p^+ = 0.11$), the values of $R(O–H)_{TS}$ and $R(H–N)_{TS}$ are 1.2932 and 1.1951 Å, respectively.

In the gas phase, the pre-TS was more stable than the reactants because the intramolecular hydrogen-bond was formed, and every reactions was endothermic; only for **4**, the higher reactive compound, was exothermic.

The calculated $\Delta H_{ts\text{-}pre}$ values associated with the reactions of **2**, **4**, and **6** are in very good agreement with the experimental activity observed (**4** > **2** ∼ **6**).

The reaction path of **5** shows two pre-TS. The first was located a *R*(H–N) 3.2132 Å and has the intramolecular hydrogen bond (OH—OCH_3) observed in neutral molecule of **5** (Figure S11). The second pre-TS a *R*(H–N) 2.3983 Å does not have this bond and the *o*-anisyl group was rotated 55.2° about the first pre-TS (φ (C_2–$C_{1'}$–C_3–C_4) is 47.60° and 102.42°, respectively). The calculated $\Delta H_{ts\text{-}pre}$ value of **5** reaction is higher than of **4** reaction.

Figure 5 displays the singly occupied molecular orbital (SOMO) and a low-lying doubly occupied molecular orbital (highest-occupied molecular orbital (HOMO), which are representative of the orbitals of TSs involving other *p*-substituted compounds. The orbitals revealed that the transferring H atom interacts with both the singly occupied p-type orbital on N· and with the lone-pair orbital on the N·.

In the TS of **1**, a different distribution was observed in the HOMO and SOMO (see Figure 5b). These results and the geometric parameters of TS (for example φ (H–O–C_4–C_3) = 16.94° for **1** and ∼−60° for **2**, **4** and **6**, Table 3) show differences with those observed for 3-(*p*-aryl) substituted and indicate a greater contribution of PCET mechanism for **1** and **8**.

Finally, different types of TSs for substituted and unsubstituted coumarins were found indicating a different contribution of HAT and PCET mechanisms, a fact that could explain the results found in the correlation between BDE and EC_{50}.

Table 3
Energy values and structural parameters of pre-TS and TS.

	2	4	6	7	5	1	8
$\Delta H_{reaction}$	2.43	−0.65	1.83	6.38	5.96	7.90	6.86
ΔH_{pre}	−2.74	−3.19	−3.66	−3.09	−1.38	−6.42	−5.94
$\Delta H_{ts\text{-}pre}$	10.33	9.68	10.31	10.50	14.03	11.81	13.36
Pre-TS							
R(O–H)	0.9779	0.9785	0.9767	0.9775	0.9775	0.9864	0.9826
R(H–N)	2.2566	2.2567	2.4193	2.2524	2.3983	1.9139	1.9411
φ (H–O–C_4–C_3)	−8.11	−11.12	−5.66	−2.07	−0.48	0.109	−1.98
θ (O–H–N·)	133.92	140.76	132.74	134.82	117.15	162.68	160.01
φ ($C_{1'}$–C_3–N·–N)	−122.52	−107.24	−142.37	−113.67	49.41	35.89	27.12[a]
φ ($C_{2'}$–$C_{1'}$–C_3–C_4)	131.06	126.30	131.49	112.89	102.42		
TS							
R(O–H)	1.2764	1.2315	1.2932	1.3373	1.2462	1.3824	1.3173
R(H–N)	1.2079	1.2512	1.1951	1.1579	1.2383	1.1365	1.1864
φ (H–O–C_4–C_3)	−61.12	−58.21	−62.03	20.49	−41.17	16.94	14.08
θ (O–H–N·)	171.45	169.91	171.52	165.33	158.78	168.21	168.83
φ ($C_{1'}$–C_3–N·–N)	−129.19	−123.50	−128.96	−103.81	25.43	11.59	67.69
φ ($C_{2'}$–$C_{1'}$–C_3–C_4)	140.72	144.20	141.67	113.54	130.52		

[a] φ (H–C_8–N·–N).

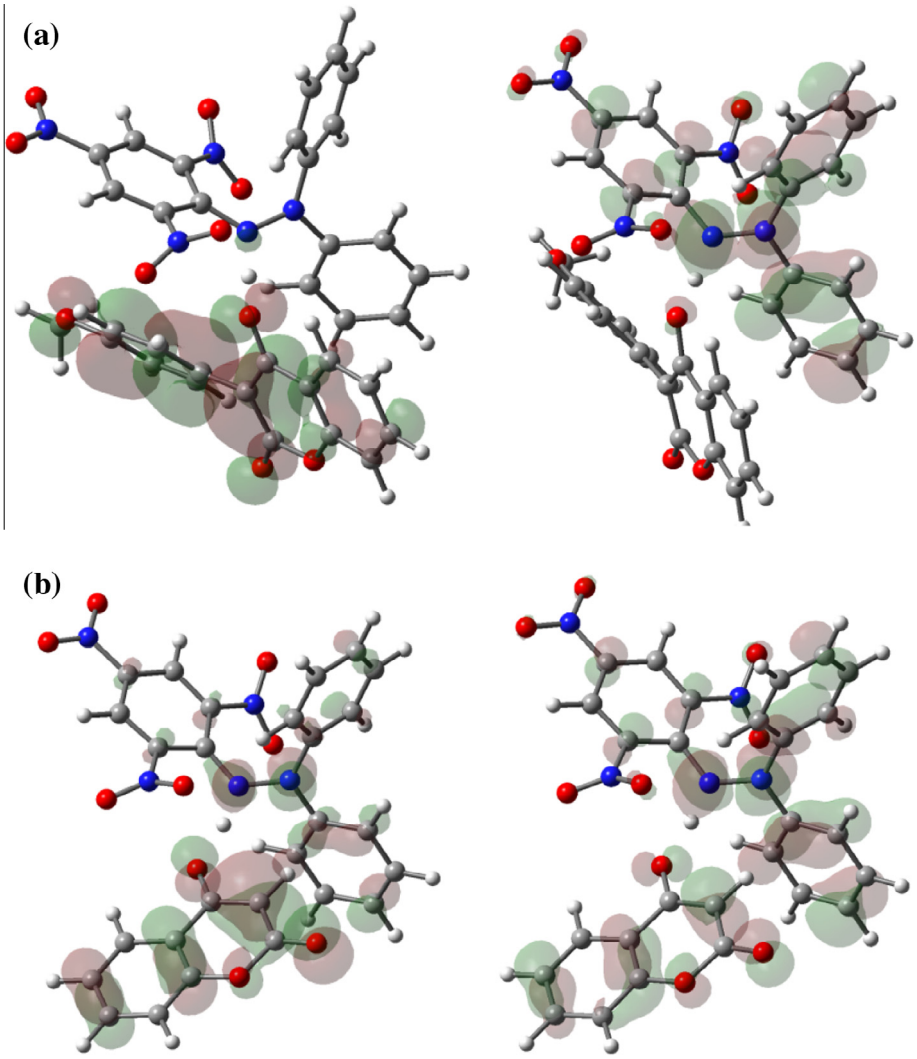

Figure 5. Molecular orbitals (SOMO and HOMO) of TS of (a) **4**, (b) **1**.

4. Conclusions

The present study assesses the main mechanisms in the reactions of a series of 4-hydroxycoumarins (no-phenolic antioxidant) with DPPH radical. In 4-hydroxycoumarins, the hydroxyl group is bound to a vinylic carbon.

It has been found that the reaction occurs by a mechanism that is substantially HAT, via a single pathway reaction. This behavior is similar to that already known for phenols.

Theoretical studies carried out in gas phase and solvent showed that the antioxidant activity can be correlated with the BDE. In the BDE, the influence of the phenyl group at position 3 is observed. Moreover, the substituents of this group have a similar effect to that observed in phenols. Therefore, both the type of substituent and its position in the phenyl group at the OH bond strength are important.

In the reaction, the mechanism can be described as a process in which the O–H hydrogen is transferred to the radical through the pre-TS with an intermolecular bond OH–N. Both the pre-TS and TS show the importance of the steric effect.

The results obtained in this study provide a physicochemical understanding of the hydrogen abstraction of a no-phenolic series of compound.

Acknowledgments

This work was supported by Consejo Nacional de Investigaciones Científicas y Técnicas (CONICET) of Argentina, SECYT UNC and CICYT-UNSE. S.A.R. acknowledges for his post-doctoral fellowship granted by CONICET.

Appendix A. Supplementary data

Supplementary data associated with this article can be found, in the online version, at http://dx.doi.org/10.1016/j.cplett.2014.03.080.

References

[1] (a) M.C. Foti, C. Daquino, Chem. Commun. 30 (2006) 3252;
(b) M.C. Foti, C. Daquino, C. Geraci, J. Org. Chem 69 (2004) 2309;
(c) G. Litwinienko, K.U. Ingold, J. Org. Chem. 68 (2003) 3433;
(d) G. Litwinienko, K.U. Ingold, J. Org. Chem. 69 (2004) 5888;
(e) G. Litwinienko, K.U. Ingold, J. Org. Chem. 70 (2005) 8982;
(f) P. Astolfi, L. Greci, T. Paul, K.U. Ingold, J. Chem. Soc., Perkin Trans. II (9) (2001) 1631.
[2] (a) S. Goldschmidt, K. Renn, Ber. Chem. 55B (1922) 628;
(b) R.I. Walter, J. Am. Chem. Soc. 88 (1966) 1930.
[3] G. Litwinienko, K.U. Ingold, Acc. Chem. Res. 40 (2007) 222.

[4] (a) J.M. Mayer, D.A. Hrovat, J.L. Thomas, W.T. Borden, J. Am. Chem. Soc. 124 (2002) 11142;
(b) G.A. DiLabio, E.R. Johnson, J. Am. Chem. Soc. 129 (2007) 6199;
(c) O. Tishchenko, D.G. Truhlar, A. Ceulemans, M.T. Nguyen, J. Am. Chem. Soc. 130 (2008) 7000.
[5] R.E. Galian, G. Litwinienko, J. Perez-Prieto, K.U. Ingold, J. Am. Chem. Soc. 129 (2007) 9280.
[6] J.S. Wright, E.R. Johnson, G.A. DiLabio, J. Am. Chem. Soc. 123 (2001) 1173.
[7] M.C. Foti, C. Daquino, I.D. Mackie, G.A. DiLabio, K.U. Ingold, J. Org. Chem. 73 (2008) 9270.
[8] S.A. Rodríguez, M.T. Baumgartner, Tetrahedron Lett. 51 (2010) 5322.
[9] S.A. Rodríguez, M.A. Nazareno, M.T. Baumgartner, Bioorg. Med. Chem. 19 (2011) 6233.
[10] Gaussian 03, Revision B.04, M. J. Frisch et al., Gaussian Inc, Pittsburgh PA, 2003.
[11] (a) C. Lee, W. Yang, R.G. Parr, Phys. Rev. B37 (1988) 785;
(b) A.D. Becke, J. Chem. Phys. 98 (1993) 1372;
(c) P.J. Stevens, F.J. Devlin, C.F. Chabalowski, M.J. Frisch, J. Phys. Chem. 98 (1994) 11623.
[12] J. Rimarčik, V. Lukeš, E. Klein, M. Ilčin,, J. Mol. Struct. (THEOCHEM) 952 (2010) 25.
[13] (a) B. Mennucci, R. Cammi, J. Tomasi, J. Chem. Phys. 110 (1999) 6858;
(b) M. Cossi, G. Scalmani, N. Rega, V. Barone, J. Chem. Phys. 117 (2002) 43.
[14] Gaussian 09, Revision B.01, M. J. Frisch et al., Gaussian Inc, Wallingford CT, 2010.
[15] The effective concentration of coumarin derivates to reduce the 50% of the radical concentration (EC_{50}) see Ref. [9].
[16] Figure S1 shows the optimized geometries of all neutral compounds and the most relevant tautomeric forms.
[17] (a) E. Klein, V. Lukes, M. Ilcin, Chem. Phys. 336 (2007) 51;
(b) E. Klein, V. Lukes, J. Mol. Struct. (Theochem) 767 (2006) 43.
[18] G. Brigati, M. Lucarini, V. Mugnaini, G.F. Pedulli, J. Org Chem. 67 (2002) 4828.
[19] (a) J.S. Wright, D.J. Carpenter, D.J. McKay, K.U. Ingold, J. Am. Chem. Soc. 119 (1997) 4245;
(b) R. Amorati, G.F. Pedulli, L. Valgimigli, H. Johansson, L. Engman, Org. Lett. 12 (2010) 2326.
[20] R. Amorati, S. Menichetti, E. Mileo, G.F. Pedulli, C. Viglianisi, Chem. Eur. J. 15 (2009) 4402.
[21] A.M. Ferrari, M. Sgobba, M.C. Gamberini, Eur. J. Med. Chem. 42 (2007) 1028;
J. Seixas de Melo, P. Fernandes, J. Mol. Struct. 565 (2001) 69.
[22] Addition of small quantities of acetic acid did not cause any appreciable decay of DPPH· within the time of reaction.
[23] *For **2***: $\Delta H_{gas}(4)$ =107.6 kcal/mol; $\Delta H_s(4)$ =34.5 kcal/mol; $\Delta H_{gas}(5)$ = −105.1 kcal/mol; $\Delta H_s(5)$ = −30.2 kcal/mol. *For **4***: $\Delta H_{gas}(4)$ = 97.5 kcal/mol; $\Delta H_s(4)$ = 27.2 kcal/mol; $\Delta H_{gas}(5)$ = −98.2 kcal/mol; $\Delta H_s(5)$ = −26.4 kcal/mol.
[24] The ideal PCET (HAT) pre-reaction complex structure would have θ (O–H–N) = 180° (180°), φ (H–O–C–C) = 0° (90°), φ (H–C–N–N)=0° (90°), and the hydroxyaryl ring co-planar with (perpendicular to) the C–N–N plane.
[25] The '*ideal*' PCET (HAT) pre-TS and TS structure would have θ (O–H–N·) = 180° (180°), φ (H–O–C–C) = 0° (90°), and φ (HC–N·–N) = 0° (90°), and the phenolic ring co-planar with (perpendicular to) the C–N·–N plane.
[26] T. Yoshida, K. Hirozumi, M. Harada, S. Hitaoka, H. Chuman J. Org Chem. 76 (2011) 4564.
[27] C. Hansch, A. Leo, R.W. Taft, Chem. Rev. 91 (1991) 165.